

## Supporting Information

# Lithium-ion storage performances of sunflower-like and nano-sized hollow SnO<sub>2</sub> spheres by spray pyrolysis and the nanoscale

## Kirkendall effect

Gi Dae Park<sup>a</sup>, Jong Hwa Kim<sup>b</sup>, and Yun Chan Kang<sup>a,\*</sup>

<sup>a</sup>Department of Materials Science and Engineering, Korea University, Anam-dong, Seongbuk-gu, Seoul 136-713, Republic of Korea

E-mail: [yckang@korea.ac.kr](mailto:yckang@korea.ac.kr) Fax: +82-2-928-3584

<sup>b</sup>Daegu Center, Korea Basic Science Institute, 80 Daehakro Bukgu, Daegu 702-701, Republic of Korea

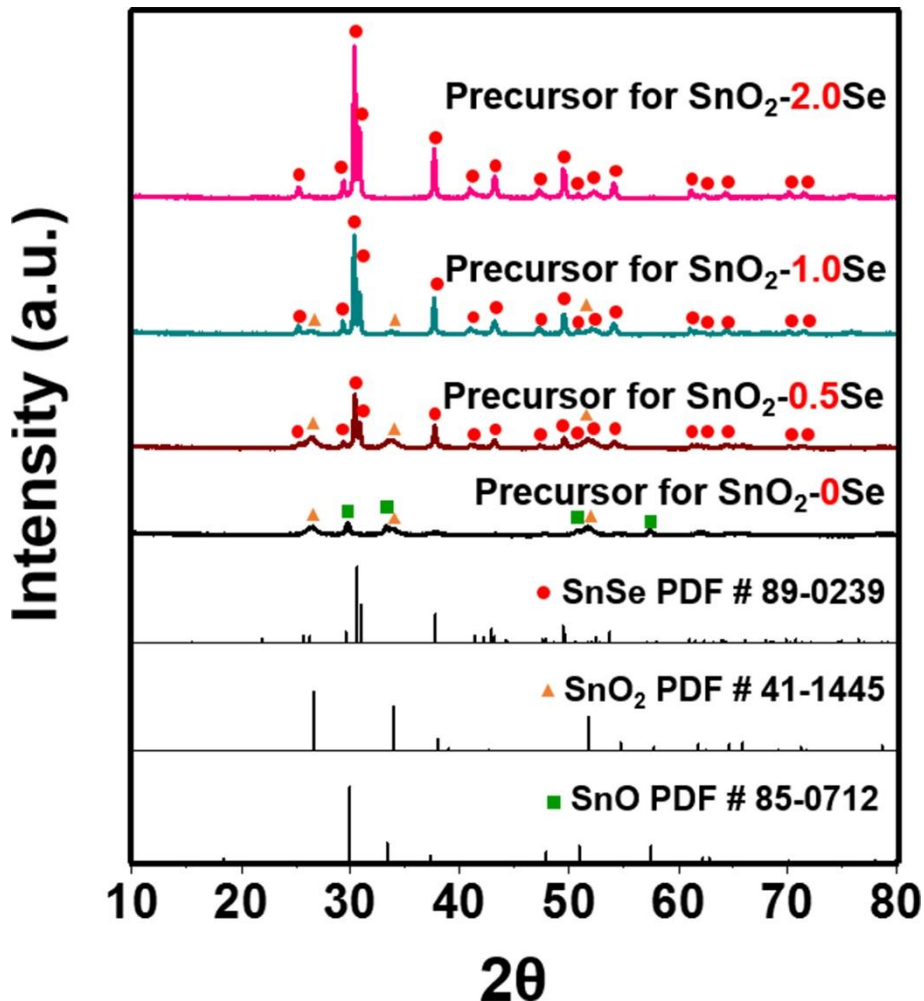


**Fig. S1** XRD patterns of precursor for SnO<sub>2</sub>-0Se, SnO<sub>2</sub>-0.5Se, SnO<sub>2</sub>-1.0Se, and SnO<sub>2</sub>-2.0Se directly formed by spray pyrolysis.

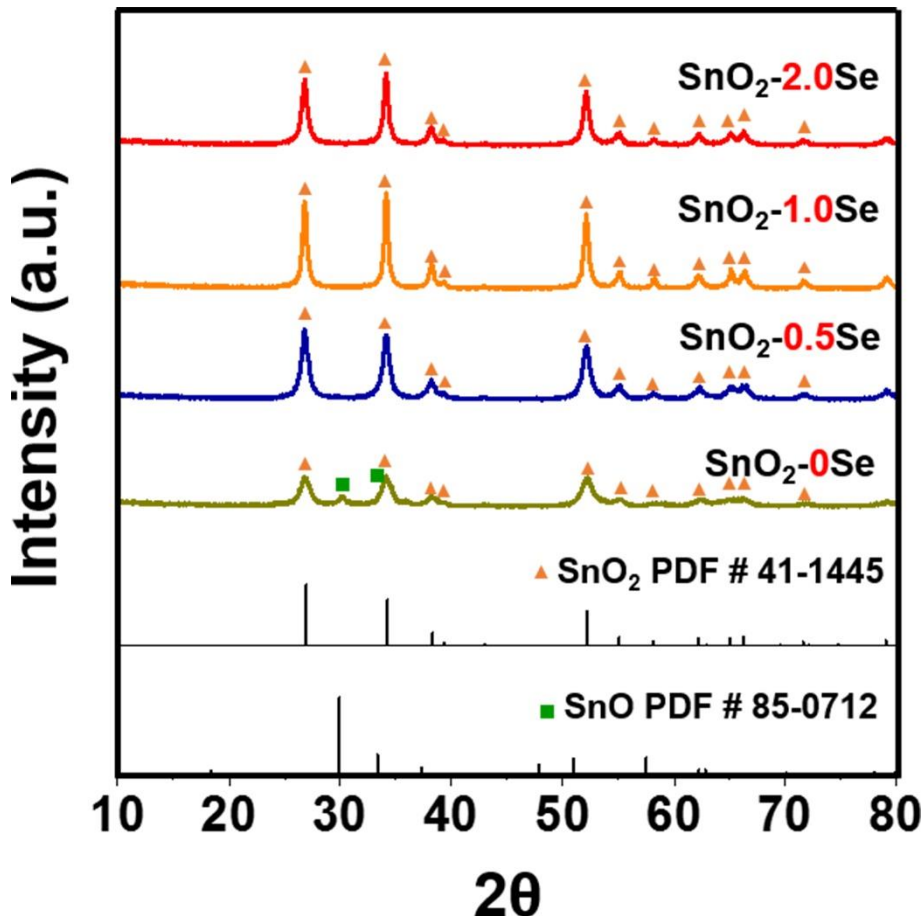


**Fig. S2** XRD patterns of  $\text{SnO}_2\text{-}0\text{Se}$ ,  $\text{SnO}_2\text{-}0.5\text{Se}$ ,  $\text{SnO}_2\text{-}1.0\text{Se}$ , and  $\text{SnO}_2\text{-}2.0\text{Se}$  formed by spray pyrolysis and subsequent oxidation process.

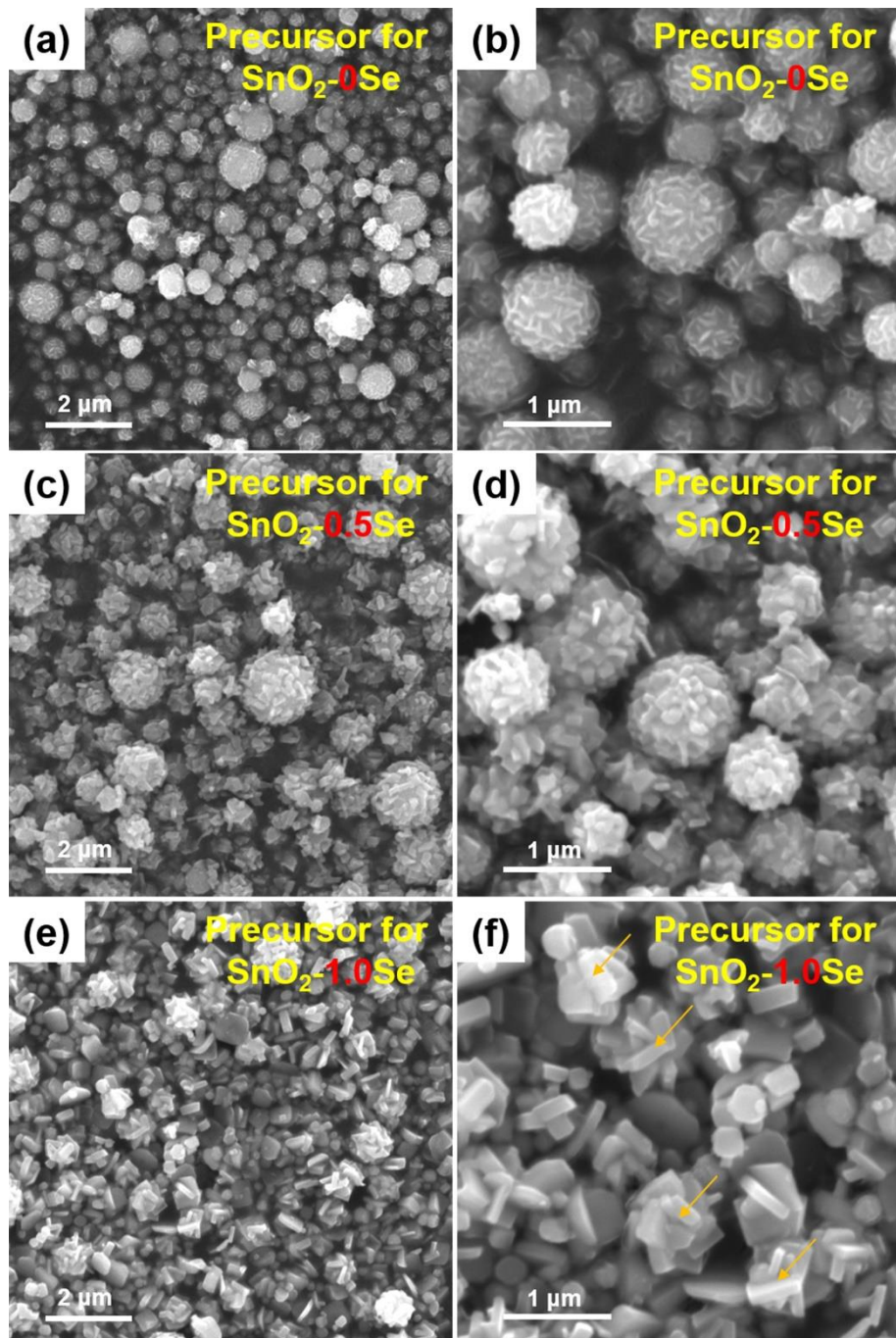


**Fig. S3** SEM images of precursor for  $\text{SnO}_2\text{-}0\text{Se}$ ,  $\text{SnO}_2\text{-}0.5\text{Se}$ , and  $\text{SnO}_2\text{-}1.0\text{Se}$  directly formed by spray pyrolysis.

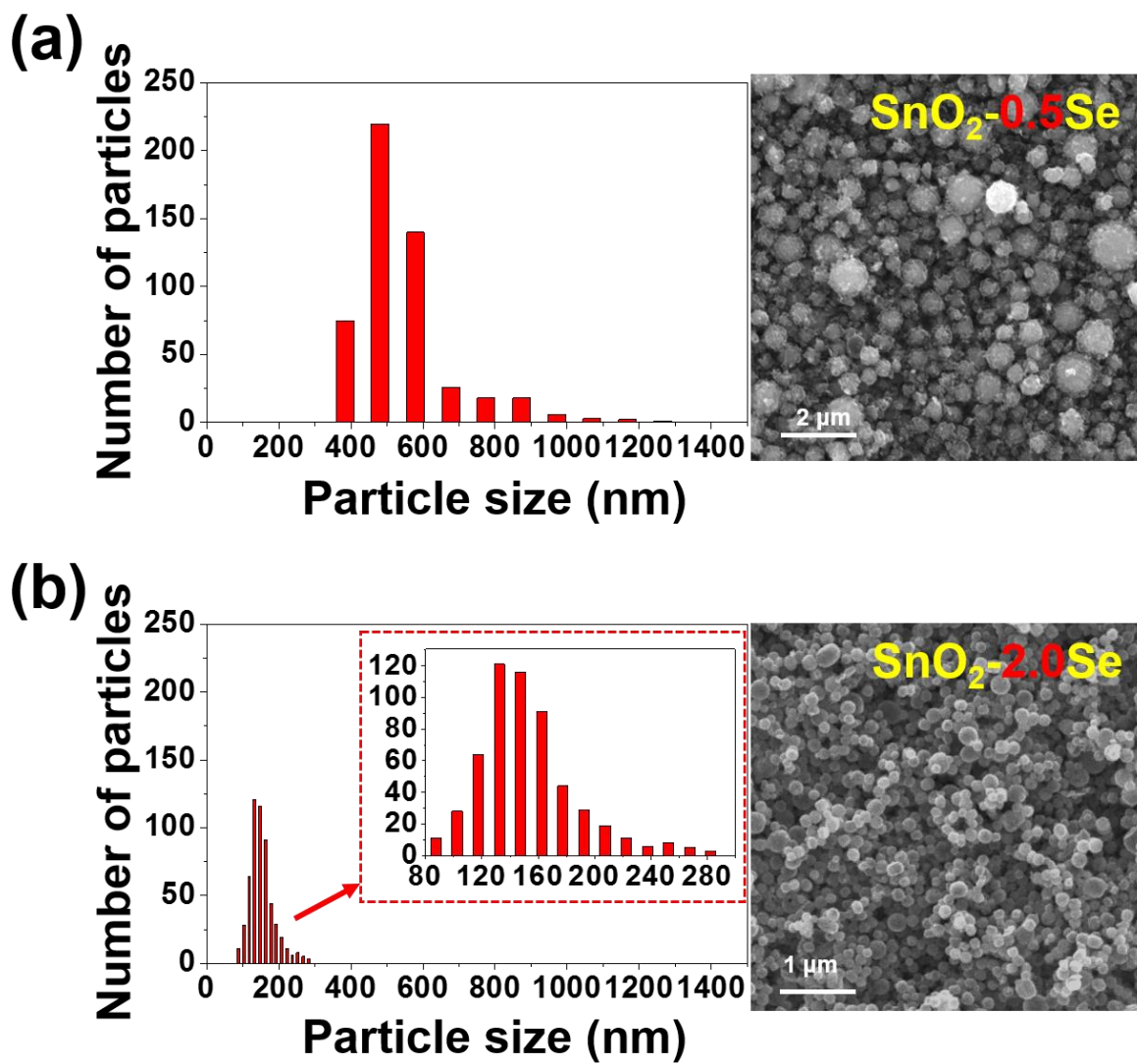


**Fig. S4** Particle size distributions of (a) SnO<sub>2</sub>-0.5Se and (b) SnO<sub>2</sub>-2.0Se samples.

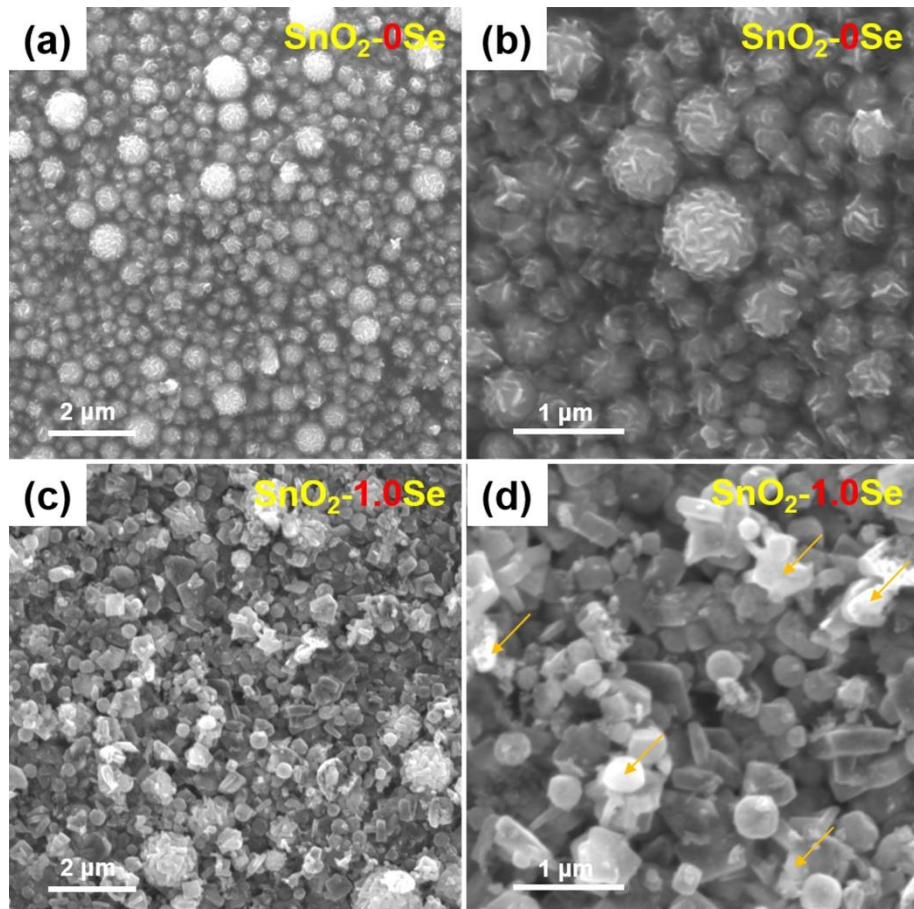


**Fig. S5** SEM images of SnO<sub>2</sub>-0Se and SnO<sub>2</sub>-1.0Se formed by spray pyrolysis and subsequent oxidation process.

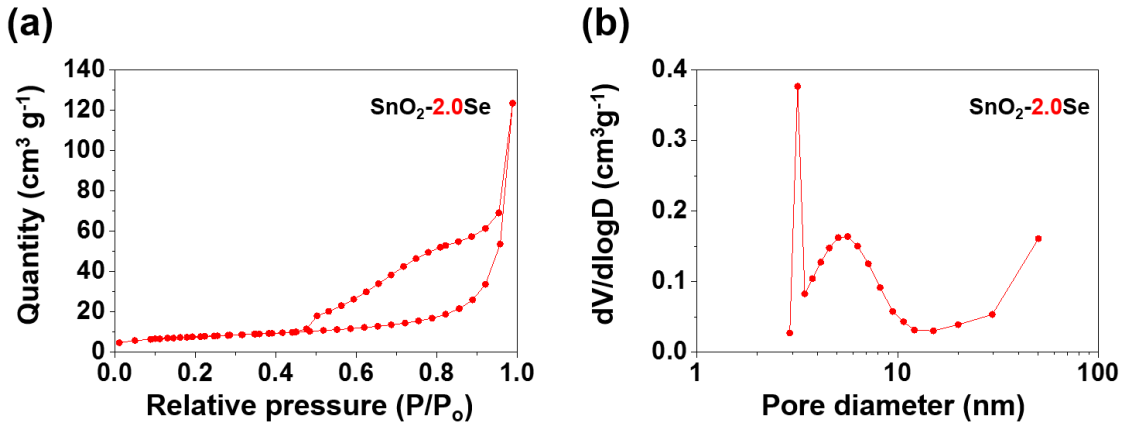
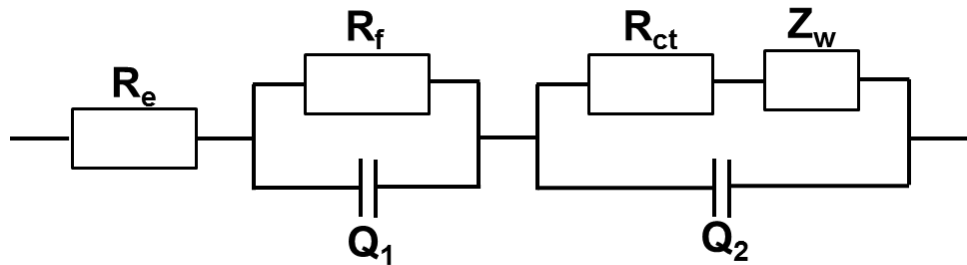


**Fig. S6** (a) N<sub>2</sub> gas adsorption and desorption isotherm and (b) BJH pore size distribution of hollow SnO<sub>2</sub> nanospheres (SnO<sub>2</sub>-2.0Se).



$R_e$  : the electrolyte resistance, corresponding to the intercept of high frequency semicircle at  $Z_{re}$  axis

$R_f$  : the SEI layer resistance corresponding to the high-frequency semicircle

$Q_1$  : the dielectric relaxation capacitance corresponding to the high-frequency semicircle

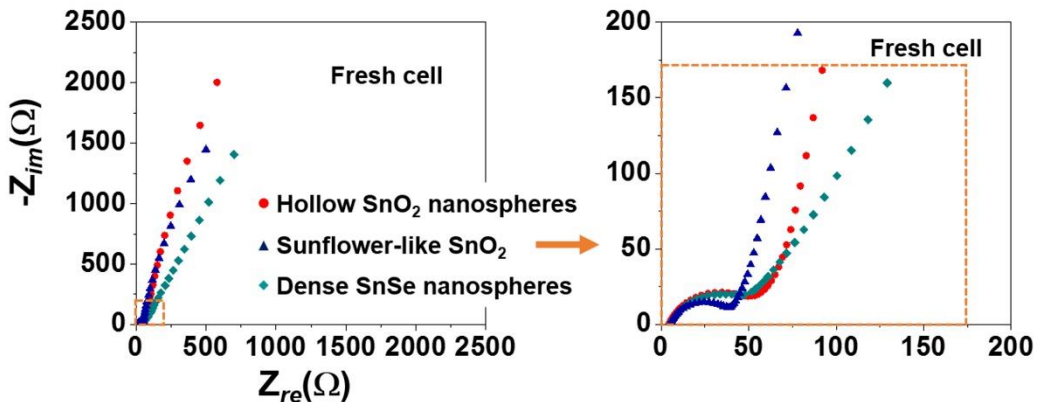
$R_{ct}$ : denote the charger transfer resistance related to the middle-frequency semicircle

$Q_2$  : the associated double-layer capacitance related to the middle-frequency semicircle

$Z_w$  : the Li-ion diffusion resistance

**Fig. S7** Randle-type equivalent circuit model used for ac impedance fitting.

(a)



(b)

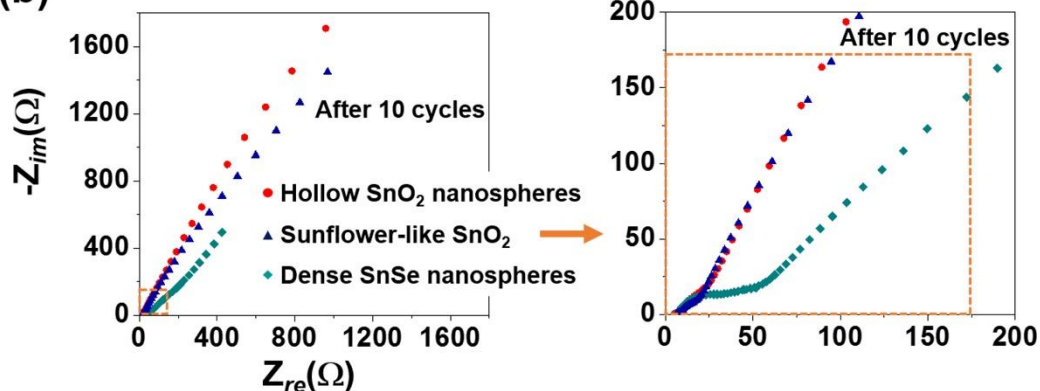


**Fig. S8** Nyquist plots of dense  $\text{SnSe}$  nanospheres (precursor powders for  $\text{SnO}_2\text{-}2.0\text{Se}$ ), sunflower-like  $\text{SnO}_2$  ( $\text{SnO}_2\text{-}0.5\text{Se}$ ), hollow  $\text{SnO}_2$  nanospheres ( $\text{SnO}_2\text{-}2.0\text{Se}$ ) : (a) fresh cell, (b) after 10 cycles.

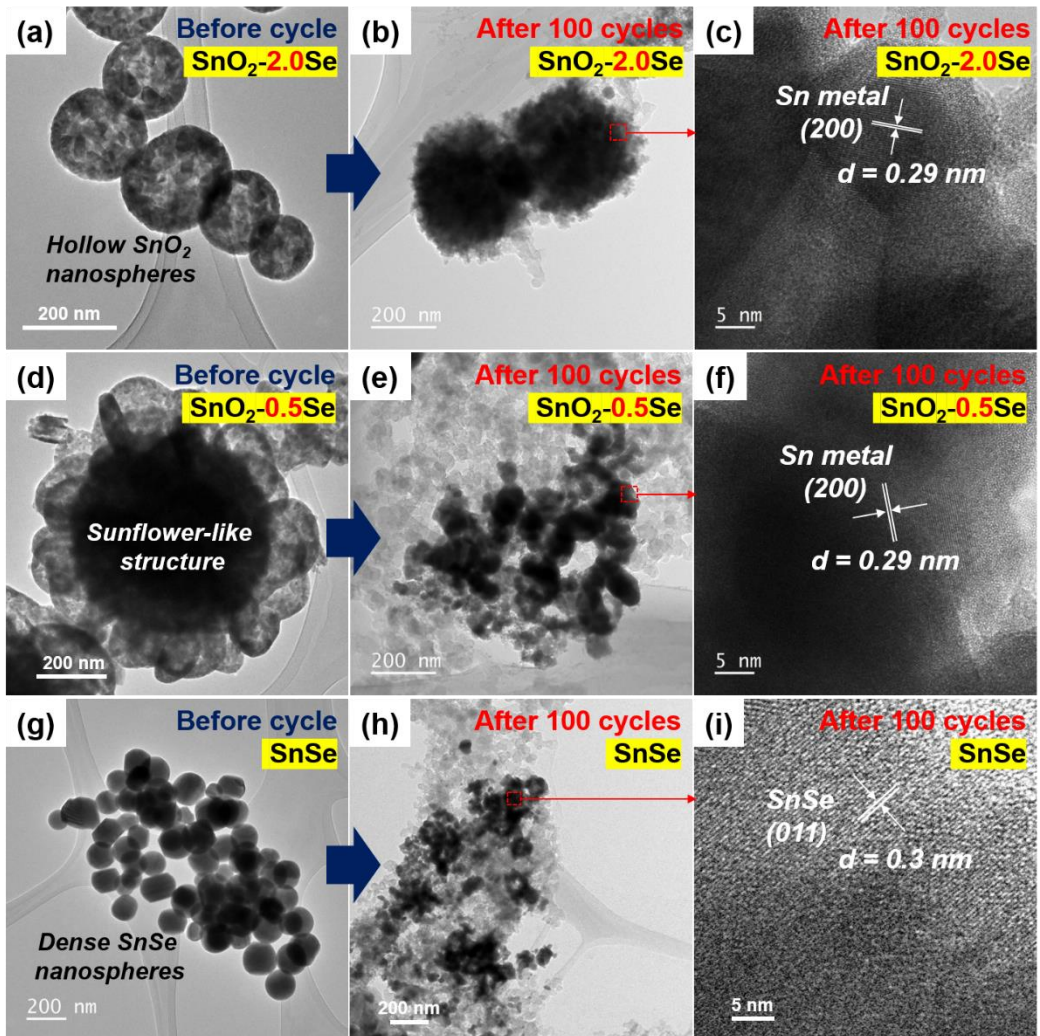


**Fig. S9** TEM images of SnO<sub>2</sub>-2.0Se, SnO<sub>2</sub>-0.5Se, and SnSe before and after 100 cycles : (a-c) SnO<sub>2</sub>-2.0Se, (d-f) SnO<sub>2</sub>-0.5Se, and (g-i) SnSe.

**Table S1.** Electrochemical performances of various nanostructured SnO<sub>2</sub> materials applied as lithium-ion batteries reported in the previous literatures.

Various hollow SnO <sub>2</sub> materials	Potential range (V)	Current density [A g <sup>-1</sup> ]	Discharge capacity [mA h g <sup>-1</sup> ] (cycle number)	Rate capacity [mA h g <sup>-1</sup> ] (Current rate [A g <sup>-1</sup> ])	Ref
SnO <sub>2</sub> hollow spheres	0.001-1.0	2.0	643 (300)	597 (7.0)	[S1]
SnO <sub>2</sub> @carbon hollow spheres	0-3.0	0.5	460 (100)	210 (3.0)	[S2]
Carbon-coated SnO <sub>2</sub> hollow spheres	0-3.0	0.1	900 (50)	670 (2.0)	[S3]
SnO <sub>2</sub> fiber-in-tube	0.001-1.0	1.0	640 (300)	591 (5.0)	[S4]
N-doped carbon-coated SnO <sub>2</sub>	0.001-2.0	0.5	491 (100)	256 (5.0)	[S5]
submicroboxes					
SnO <sub>2</sub> hollow nanostructures	0.001-2.0	0.1	540 (50)	460 (7.8)	[S6]
SnO <sub>2</sub> -carbon composite microspheres	0.001-1.2	1.5	509 (1000)	389 (9.0)	[S7]
Carbon nanotube @SnO <sub>2</sub> -Au coaxial nanocable	0.01-1.2	0.18	626 (40)	392 (7.2)	[S8]
SnO <sub>2</sub> -C hollow nanostructures	0.01-3.0	0.2	577 (500)	415 (5.0)	[S9]
SnO <sub>2</sub> hollow nanoplates	0.01-1.0	1.0	635 (300)	267 (30.0)	[S10]
Mesoporous SnO <sub>2</sub> nanowire	0-1.2	0.4	773 (50)	250 (20.0)	[S11]
<b>Hollow SnO<sub>2</sub> nanospheres</b>	<b>0.001-3.0</b>	<b>3.0</b>	<b>1043 (500)</b>	<b>638 (10.0)</b>	<b>This study</b>

## References

- [S1] J. S. Cho, H. S. Ju, Y. C. Kang, *Sci. Rep.*, 2016, **6**, 23915.
- [S2] X. W. Lou, C. M. Li, L. A. Archer, *Adv. Mater.*, 2009, **21**, 2536.
- [S3] Q. Liu, Y. Dou, B. Y. Ruan, Z. Q. Sun, S. L. Chou, S. X. Dou, *Chem. Eur. J.*, 2016, **22**, 5853.
- [S4] Y. J. Hong, J. W. Yoon, J. H. Lee, Y. C. Kang, *Chem. Eur. J.*, 2016, **21**, 371.

- [S5] X. Zhou, L. Yu, X. W. Lou, *Adv. Energy Mater.*, 2016, **6**, 1600451.
- [S6] X. M. Yin, C. C. Li, M. Zhang, Q. Y. Hao, S. Liu, L. B. Chen, T. H. Wang, *J. Phys. Chem. C.*, 2010, **114**, 8084.
- [S7] Y. N. Ko, S. B. Park, Y. C. Kang, *Small*, 2014, **10**, 3240.
- [S8] G. Chen, Z. Y. Wang, D. G. Xia, *Chem. Mater.*, 2008, **20**, 6951.
- [S9] Q. H. Tian, Y. Tian, Z. Zhang, L. Yang, S. I. Hirano, *J. Power Sources*, 2016, **306**, 213.
- [S10] G. D. Park, J.-K. Lee, Y. C. Kang, *Adv. Funct. Mater.*, 2017, **27**, 1603399.
- [S11] H. Kim, J. Cho, *J. Mater. Chem.*, 2008, **18**, 771-775.